IEICE TRANS. COMMUN., VOL.E105–B, NO.9 SEPTEMBER 2022

PAPER

PAPR Reduction of OFDM Signals Using Null Space in MIMO Channel for MIMO Amplify-and-Forward Relay Transmission*

Yuki SEKIGUCHI[†], ***Student Member***, **Nobuhide NONAKA**[††], ***Member***, ***and*** **Kenichi HIGUCHI**[†a)], ***Senior Member***

SUMMARY In this paper, we propose applying our previously reported adaptive peak-to-average power ratio (PAPR) reduction method using null space in a multiple-input multiple-output (MIMO) channel for orthogonal frequency division multiplexing (OFDM) signals to the downlink MIMO amplify-and-forward (AF) relaying transmission. Assuming MIMO-OFDM transmission, mitigating its high PAPR not only at the base station (BS) but also at the relay station (RS) transmitters is essential to achieve sufficient coverage enhancement from the RSs by minimizing the transmission power backoff levels at the nonlinear power amplifier. In this study, we assume an AF-type RS with multiple antennas. In the proposed method, the BS suppresses the PAPR of the transmitted signal through adaptive PAPR reduction utilizing the null space of the integrated overall MIMO channel that combines the channel between the BS and RS and the channel between the RS and a set of user equipment (UE). However, the PAPR of the received signal at each RS antenna is increased again due to the MIMO channel between the BS and RS. The proposed method reduces this increased PAPR at the AF-type RS transmitter by PAPR reduction processing that utilizes the null space in the MIMO channel between the RS and UE. Since the in-band PAPR reduction signal added at the RS transmitter is transmitted only in the null space of the MIMO channel between the RS and UE, interference at the UE receiver is mitigated. Computer simulation results show that the proposed method significantly improves the PAPR-vs.-throughput performance compared to that for the conventional one thanks to the reduced interference levels from the PAPR reduction signal observed at the UE receiver.

key words: *OFDM, PAPR, MIMO, null space, relaying, amplify-and-forward*

1. Introduction

The combination of massive multiple-input multiple-output (MIMO) [1], [2] using beamforming (BF) and orthogonal frequency division multiplexing (OFDM) signals offers wide-coverage enhanced mobile broadband communication. Furthermore, in the 5th generation mobile communication system New Radio (NR) [3] and beyond [4], in order to provide wireless transmission in a high frequency band such as the millimeter wave band with wide coverage, the importance of relay transmission [5]–[7] increases. In this paper, we consider downlink MIMO-OFDM transmission using amplify-and-forward (AF) type relaying. Here, the AF relay station (RS) is equipped with multiple antennas and transfers the received signal from the base station (BS) to a set of user equipment (UE) after power amplification without decoding the data signal.

The major drawback to OFDM signals is their high peak-to-average power ratio (PAPR). When a signal with a high PAPR is amplified by a power amplifier, the input signal power must be decreased in order to suppress the in-band and out-of-band distortion signals generated due to the nonlinearity of the power amplifier, which leads to a decrease in the transmission power. In massive MIMO, in which a power amplifier is prepared for each of a large number of transmitter antennas, reducing the PAPR is particularly important. This problem is the same for the RS, and PAPR reduction both at the BS and RS transmitters is very important to achieve high-speed high-quality transmission with wide coverage through relaying.

A number of PAPR reduction methods employing OFDM have been investigated, e.g., in [8]–[16]. Among these methods, when a powerful channel code such as the turbo code or low-density parity check (LDPC) code is employed, [17] revealed that the PAPR reduction method that does not reduce the frequency efficiency at the cost of in-band interference such as the clipping and filtering (CF) method [9], [10] is superior to those that consume a part of the frequency bandwidth to reduce the PAPR such as the tone reservation method [13] from the viewpoint of the tradeoff between the PAPR reduction and the error rate.

Various studies have also been conducted on PAPR reduction methods for OFDM signals in relay transmission. Basically, the PAPR reduction method described above can be applied to PAPR reduction of the OFDM signal at the RS transmitter. For example, in [18], reducing the PAPR in an RS based on CF is investigated. In [19], PAPR reduction in the RS based on a partial transmit sequence (PTS) is investigated. In [20], the PAPR reduction method applied to an RS based on the superimposition of the Golay sequence and the Reed-Muller code on the transmission signal is investigated. In either method, in-band interference and distortion occur in the received signal at the UE due to the PAPR reduction process, and the reception quality of the data signal deteriorates or complicated signal processing is required in the UE receiver to avoid this.

Members of our research group reported on a PAPR reduction method utilizing the null space in a MIMO channel for MIMO-OFDM signals [21]–[24]. Hereafter, this method

Manuscript received October 16, 2021.
Manuscript revised February 8, 2022.
Manuscript publicized March 22, 2022.

[†]The authors are with the Graduate School of Science and Technology, Tokyo University of Science, Noda-shi, 278-8510 Japan.
[††]The author is with NTT DOCOMO, INC., Yokosuka-shi, 239-8536 Japan.

*The material in this paper was presented in part at the 94th IEEE Vehicular Technology Conference (VTC2021-Fall), Online, 2021.

a) E-mail: higuchik@rs.tus.ac.jp

DOI: 10.1587/transcom.2021EBT0006

is simply referred to the adaptive PAPR reduction method. The adaptive PAPR reduction method restricts the in-band PAPR reduction signal transmitted to only the null space in the given MIMO channel to suppress the degradation in the transmission quality of the data streams due to the interference from the in-band PAPR reduction signal. Since all the transmitter antennas are fully utilized in transmitting the data streams, the achievable BF gain of the adaptive PAPR reduction method is higher than that for the method in [25]. We note that [26] investigates the unused beam reservation-based PAPR reduction method, which is similar to the method originally reported in [21] and [22] in which the null space in a MIMO channel is utilized.

In this paper, we propose a method that applies the adaptive PAPR reduction method utilizing the null space in the MIMO channel for MIMO-OFDM signal to the multi-antenna AF type RS. In the proposed method, the BS suppresses the PAPR of the transmitted signal through adaptive PAPR reduction utilizing the null space of the integrated overall MIMO channel that combines the channel between the BS and RS and the channel between the RS and UE. As a result, the PAPR at the BS transmitter is suppressed, while the PAPR reduction signal transmitted from the BS is not observed at the UE receiver. Therefore, it does not interfere with the data signal. At the RS, the transmission signal in which the PAPR is suppressed once at the BS transmitter is received. However, the signals transmitted from each BS antenna are superposed via the MIMO channel between the BS and RS, and then received by the RS. Furthermore, the noise component generated at the RS receiver is added to the received signal at the RS. Therefore, the PAPR of the received signal at each RS antenna is increased again. This increased PAPR at the AF-type RS transmitter is reduced by PAPR reduction processing that utilizes the null space in the MIMO channel between the RS and UE. Since the in-band PAPR reduction signal added at the RS transmitter is transmitted only in the null space of the MIMO channel between the RS and UE, interference at the UE receiver is mitigated. Computer simulation results show the effectiveness of the proposed method from the viewpoints of the PAPR and throughput, quantitatively. We note that the contents of this paper are based on [27], but include enhanced evaluation and discussions.

The remainder of the paper is organized as follows. First, Sect. 2 describes the system model. Section 3 presents the proposed method. Section 4 presents numerical results based on computer simulations. Finally, Sect. 5 concludes the paper.

2. System Model

Figure 1 shows the system model assumed in this paper. The number of BS transmitter antennas is N_{B} and that for RS antennas is N_{R}. We consider downlink multiuser MIMO transmission where N_{U} users each having a single receiver antenna are spatially multiplexed. Assuming a typical massive MIMO environment, we set $N_{\mathrm{B}} > N_{\mathrm{R}} > N_{\mathrm{U}}$. The

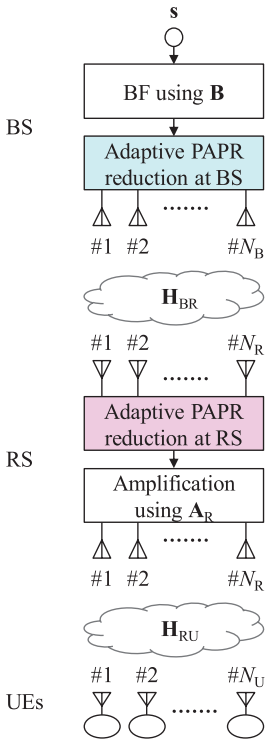

Fig. 1 System model.

$N_{\mathrm{R}} \times N_{\mathrm{B}}$-dimensional channel matrix between the BS and RS is denoted as $\mathbf{H}_{\mathrm{BR}}$. The $N_{\mathrm{U}} \times N_{\mathrm{R}}$-dimensional channel matrix between the RS and UEs is denoted as $\mathbf{H}_{\mathrm{RU}}$. In this paper, we assume that the MIMO channel is not frequency-selective for the sake of simplicity.

The N_{U}-dimensional data stream vector before BF is denoted as $\mathbf{s}$. Assuming that the $N_{\mathrm{B}} \times N_{\mathrm{U}}$-dimensional BF matrix is $\mathbf{B}$, the N_{B}-dimensional transmission signal vector after BF, $\mathbf{x}$, is expressed as $\mathbf{Bs}$. In this paper, we assume zero-forcing-based BF applied to the overall MIMO channel, $\mathbf{H}_{\mathrm{total}} = \mathbf{H}_{\mathrm{RU}}\mathbf{A}_{\mathrm{R}}\mathbf{H}_{\mathrm{BR}}$. Thus, $\mathbf{x}$ is represented as

$$\mathbf{x} = \mathbf{Bs} = \sqrt{P}\mathbf{H}_{\mathrm{total}}^{-}\mathbf{s} = \sqrt{P}\left(\mathbf{H}_{\mathrm{RU}}\mathbf{A}_{\mathrm{R}}\mathbf{H}_{\mathrm{BR}}\right)^{-}\mathbf{s}. \tag{1}$$

Here, $\sqrt{P}$ is a channel-dependent constant that is determined so that the maximum transmission power constraint holds. Matrix $\mathbf{A}_{\mathrm{R}}$ is a diagonal matrix showing the power amplification operation in the RS. It is assumed that the BS knows $\mathbf{H}_{\mathrm{total}}$ and the RS knows $\mathbf{H}_{\mathrm{RU}}\mathbf{A}_{\mathrm{R}}$ in advance.

3. Proposed Method

The proposed method applies the adaptive PAPR reduction method utilizing the null space in a MIMO channel to the BS transmitter and RS transmitter in the multi-antenna AF relay transmission system shown in Fig. 1. Since frequency selectivity of the channel is not considered in this paper, the time-domain signal at the time of interest is described in the following signal notation. As an implementation algorithm of the adaptive PAPR reduction method using the null space in the MIMO channel, two algorithms are considered: the

CF followed by the channel-null constraint (CFCNC) [21], [22] and peak cancellation (PC) signal with the channel-null constraint (PCCNC) [23], [24]. In this paper, we use CFCNC.

3.1 PAPR Reduction Process at BS

Regarding the $N_U \times N_B$-dimensional overall channel matrix, $\mathbf{H}_{total} = \mathbf{H}_{RU}\mathbf{A}_R\mathbf{H}_{BR}$, we have the $N_B \times (N_B - N_U)$-dimensional matrix, $\mathbf{V}_{total}$, which corresponds to the null space in $\mathbf{H}_{total}$, since we set $N_B > N_U$. Thus, $\mathbf{H}_{total}\mathbf{V}_{total} = \mathbf{O}$ and we assume that all column vectors of $\mathbf{V}_{total}$ are orthonormal.

The BS performs CF, which includes amplitude clipping and filtering that suppresses out-of-band distortion due to clipping, on transmission signal vector $\mathbf{x}$ with power threshold T_B. Assuming that $\mathbf{x}$ is converted to $\tilde{\mathbf{x}}$ by CF processing, $\mathbf{\Delta}_B = \tilde{\mathbf{x}} - \mathbf{x}$ corresponds to the PAPR reduction signal vector generated by CF. In the proposed method, in order to ensure that $\mathbf{\Delta}_B$ is emitted only into the null space in the overall MIMO channel, $\mathbf{\Delta}_B$ is projected onto null space $\mathbf{V}_{total}$ of the overall channel matrix, $\mathbf{H}_{total}$.

$$\tilde{\mathbf{\Delta}}_B = \mathbf{V}_{total}\mathbf{V}_{total}^H\mathbf{\Delta}_B. \tag{2}$$

The PAPR reduction effect by amplitude clipping is decreased due to the filtering operation in the CF and the projection processing onto the null space using (2). So, the CF operation and the projection of the PAPR reduction signal vector onto null space $\mathbf{V}_{total}$ are repeated L_B times, and $\mathbf{x} + \tilde{\mathbf{\Delta}}_B$ at the final iteration is transmitted.

3.2 PAPR Reduction Process at RS

After the BS transmits $\mathbf{x} + \tilde{\mathbf{\Delta}}_B$, the N_R-dimensional received signal vector at the RS, $\mathbf{y}_R$, is represented as

$$\mathbf{y}_R = \mathbf{H}_{BR}(\mathbf{x} + \tilde{\mathbf{\Delta}}_B) + \mathbf{z}_R, \tag{3}$$

where $\mathbf{z}_R$ is the noise vector observed at the RS receiver. Although the PAPR of $\mathbf{x} + \tilde{\mathbf{\Delta}}_B$ is low, the PAPR of $\mathbf{y}_R$ is increased again since $\mathbf{y}_R$ is a linear sum of all elements of $\mathbf{x} + \tilde{\mathbf{\Delta}}_B$ depending on the MIMO channel between the BS and RS, $\mathbf{H}_{BR}$. Noise $\mathbf{z}_R$ is another source of the PAPR enhancement. Therefore, in the proposed method, the PAPR reduction method using the null space in the MIMO channel is applied again to $\mathbf{y}_R$ at the RS.

The effective MIMO channel between the RS and UEs including amplification matrix $\mathbf{A}_R$ is $N_U \times N_R$-dimensional matrix $\mathbf{H}_{RU}\mathbf{A}_R$. Since we set $N_R > N_U$, we have the $N_R \times (N_R - N_U)$-dimensional matrix, $\mathbf{V}_{RU}$, which corresponds to the null space in the effective MIMO channel between the RS and UEs, $\mathbf{H}_{RU}\mathbf{A}_R$. Thus, $\mathbf{H}_{RU}\mathbf{A}_R\mathbf{V}_{RU} = \mathbf{O}$ and all column vectors of $\mathbf{V}_{RU}$ are assumed to be orthonormal.

The RS performs CF on received signal vector $\mathbf{y}_R$ with power threshold T_R. Assuming that $\mathbf{y}_R$ is converted to $\tilde{\mathbf{y}}_R$ by CF, $\mathbf{\Delta}_R = \tilde{\mathbf{y}}_R - \mathbf{y}_R$ corresponds to the PAPR reduction signal vector generated by CF at the RS. In the proposed method, in order to ensure that $\mathbf{\Delta}_R$ is emitted only into the null space in the effective MIMO channel between the RS and UEs, $\mathbf{\Delta}_R$ is projected onto null space $\mathbf{V}_{RU}$ of effective channel matrix $\mathbf{H}_{RU}\mathbf{A}_R$.

$$\tilde{\mathbf{\Delta}}_R = \mathbf{V}_{RU}\mathbf{V}_{RU}^H\mathbf{\Delta}_R. \tag{4}$$

The PAPR reduction effect by amplitude clipping is decreased due to the filtering operation in the CF and the projection processing onto the null space using (4). So, the CF operation and the projection of the PAPR reduction signal vector onto null space $\mathbf{V}_{RU}$ are repeated L_R times, and $\mathbf{y}_R + \tilde{\mathbf{\Delta}}_R$ at the final iteration is amplified and forwarded as $\mathbf{x}_R = \mathbf{A}_R(\mathbf{y}_R + \tilde{\mathbf{\Delta}}_R)$.

3.3 Received Signal at UEs

From the above, the received signal vector, $\mathbf{y}_U$, in N_U UEs in the proposed method is expressed by the following equation.

$$\begin{aligned}
\mathbf{y}_U &= \mathbf{H}_{RU}\mathbf{x}_R + \mathbf{z}_U = \mathbf{H}_{RU}\mathbf{A}_R\left(\mathbf{y}_R + \tilde{\mathbf{\Delta}}_R\right) + \mathbf{z}_U \\
&= \mathbf{H}_{RU}\mathbf{A}_R\mathbf{y}_R + \mathbf{H}_{RU}\mathbf{A}_R\mathbf{V}_{RU}\mathbf{V}_{RU}^H\mathbf{\Delta}_R + \mathbf{z}_U \\
&= \mathbf{H}_{RU}\mathbf{A}_R\left(\mathbf{H}_{BR}\left(\mathbf{x} + \tilde{\mathbf{\Delta}}_B\right) + \mathbf{z}_R\right) + \mathbf{z}_U \\
&= \mathbf{H}_{RU}\mathbf{A}_R\mathbf{H}_{BR}\mathbf{x} + \mathbf{H}_{RU}\mathbf{A}_R\mathbf{H}_{BR}\mathbf{V}_{total}\mathbf{V}_{total}^H\mathbf{\Delta}_B \\
&\quad + \mathbf{H}_{RU}\mathbf{A}_R\mathbf{z}_R + \mathbf{z}_U \\
&= \mathbf{H}_{RU}\mathbf{A}_R\mathbf{H}_{BR}\sqrt{P}\left(\mathbf{H}_{RU}\mathbf{A}_R\mathbf{H}_{BR}\right)^{-}\mathbf{s} + \mathbf{H}_{RU}\mathbf{A}_R\mathbf{z}_R + \mathbf{z}_U \\
&= \sqrt{P}\mathbf{s} + \mathbf{H}_{RU}\mathbf{A}_R\mathbf{z}_R + \mathbf{z}_U.
\end{aligned} \tag{5}$$

Vector $\mathbf{z}_U$ is the noise vector observed at the UE receivers. Therefore, in the proposed method, the PAPR reduction signal generated by the BS and RS does not appear in the received signal of the UE, so that the PAPR reduction can be actualized at the BS and RS transmitters while abating the deterioration in throughput.

4. Numerical Results

4.1 Simulation Parameters

The performance of the proposed method is evaluated based on computer simulations. Table 1 gives the major simulation parameters. The number of BS transmitter antennas, N_B, is set to 128. The number of RS antennas, N_R, and the number of UEs, N_U, are parameterized. The number of OFDM signal subcarriers is 512. The number of fast Fourier transform (FFT)/inverse FFT (IFFT) points is set to 2048, which corresponds to four-times oversampling in the time domain in order to measure the PAPR levels accurately [28]. For evaluation generality, we assume that the symbol constellation of each subcarrier follows an independent standard complex Gaussian distribution. Zero-forcing BF is applied. As the channel model, we assume flat Rayleigh fading, which is independent between any pairs of transmitter and receiver antenna branches. As for power amplification matrix $\mathbf{A}_R$ at the RS, $\mathbf{A}_R$ is set to be an identity matrix assuming a common amplification gain for all N_R antennas, except in Figs. 11 and

Table 1 Simulation parameters.

Number of BS antennas, N_B		128
Number of RS antennas, N_R		Parameterized
Number of UEs, N_U		Parameterized
Number of subcarriers		512
Number of FFT/IFFT points		2048
Constellation of data modulation		i.i.d. complex Gaussian distributed
BF		Zero-forcing
Channel model		Flat Rayleigh No fading correlations between any pair of transmitter and receiver antennas
SNR	Between BS and RS	10 dB
	Between RS and UEs	10 dB
Throughput calculation		Shannon formula where the Bussgang theorem is taken into account

12 where the amplification gain of each antenna at the RS is channel-dependently controlled so that the transmission power levels of all antennas are equalized. The signal-to-noise ratio (SNR) is set to 10 dB between the BS and RS and between the RS and all UEs. The PAPR is defined as the ratio of the peak signal power to the average signal power across all the transmitter antennas per OFDM symbol. The power thresholds, T_B and T_R, in the PAPR reduction process are defined as the signal power threshold normalized by the signal power per antenna averaged over the channel realizations. The sum throughput of N_U streams (users) is calculated based on the Shannon formula considering the Bussgang theorem [29]. The numbers of iterations in the proposed CFCNC at the BS and RS, L_B and L_R, respectively, are parameterized.

4.2 Simulation Results

Figure 2 shows the complementary cumulative distribution function (CCDF) of the PAPR before and after the PAPR reduction process at the BS and RS. For both the BS and RS, the proposed adaptive PAPR reduction method utilizing the null space in the MIMO channel is applied. The number of RS antennas, N_R, and the number of UEs, N_U, are 64 and 4, respectively. Power thresholds T_B and T_R in the PAPR reduction at the BS and RS are both set to 7 dB. The numbers of iterations of adaptive PAPR reduction using CFCNC at the BS and RS, L_B and L_R are both set to 20. Figure 2 shows that the PAPR of the BS transmission signal is significantly reduced by the PAPR reduction process, but returns to a high PAPR when it is received by the RS. This is because the transmission signals of the N_B of 128 BS antennas after PAPR reduction are received at each of the N_R = 64 RS antennas in a superposed manner via the MIMO channel. In addition, the influence of noise at the RS receiver is added. We note that the PAPR of the received signal before PAPR reduction at the RS is distributed at a value approximately 1 dB lower than that for the PAPR of the transmission signal before PAPR reduction at the BS. This is because the number of RS antennas, N_R, is set to 1/2 that of the BS antennas, N_B, in this evaluation. This reduces the variation in signal power between the antennas at the RS receiver. To confirm this, Fig. 3 shows the CCDF of the PAPR when N_R is set

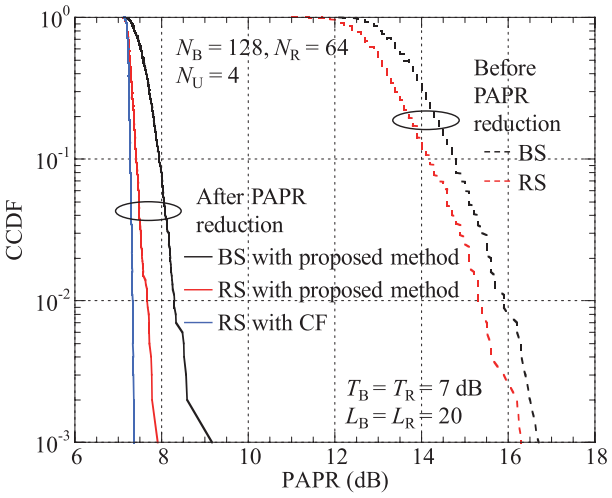

Fig. 2 CCDF of PAPR when N_R = 64.

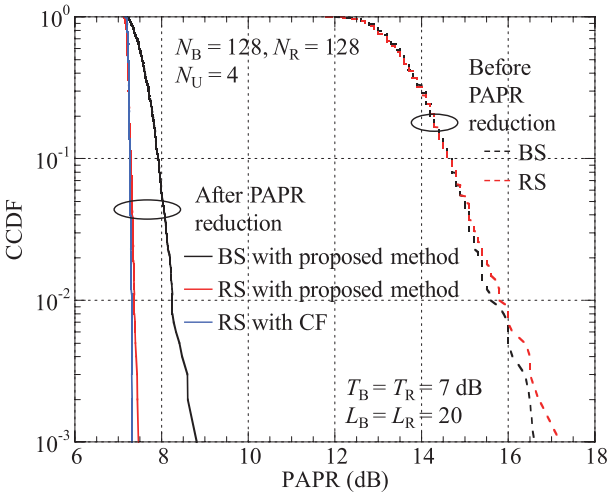

Fig. 3 CCDF of PAPR when $N_R = N_B = 128$.

equal to N_B = 128. We see that the distribution of the PAPR of the received signal before PAPR reduction at the RS becomes close to that of the transmission signal before PAPR reduction at the BS when $N_R = N_B$. From Figs. 2 and 3, we confirm that sufficient PAPR reduction processing is required at the RS as well as at the BS in a MIMO-relaying scenario.

In Figs. 2 and 3, the PAPR at the RS is lower than that at the BS after PAPR reduction. The reason for this can be explained by using the analysis presented in [30]. Based on [30], in order for the adaptive PAPR reduction method utilizing the null space in the MIMO channel to work well, the cross correlation of the transmission signal among antennas must be as low as possible. Since channel $\mathbf{H}_{BR}$ randomizes the received signals at the RS antennas, the cross correlation of the received signals among the RS antennas becomes lower than that for the transmission signals among the BS transmitter antennas. For example, in Fig. 3 where $N_B = N_R = 128$, the average of the normalized squared cross

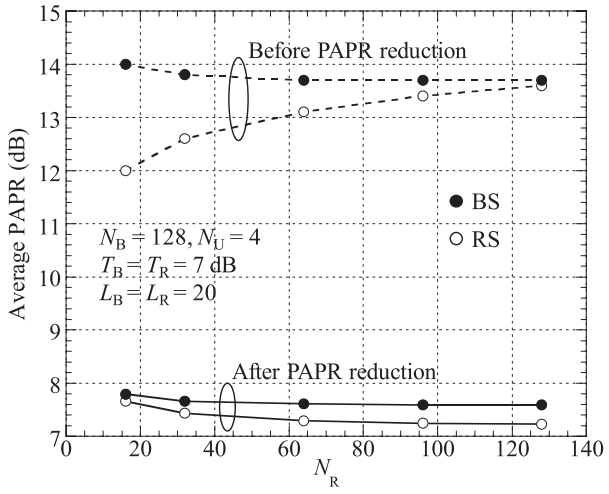

Fig. 4 Average PAPR as a function of N_R.

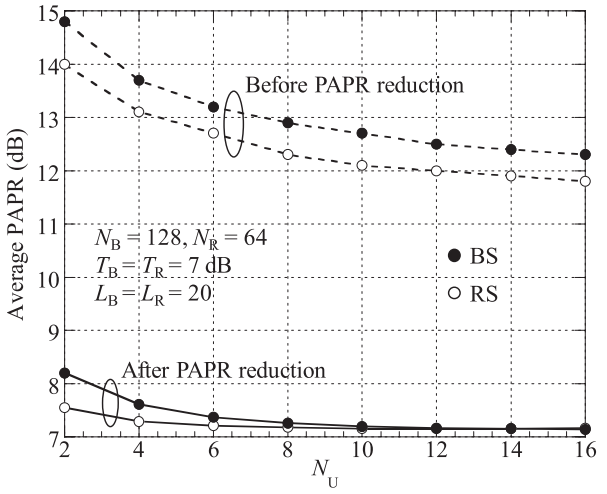

Fig. 5 Average PAPR as a function of N_U.

correlation of the transmission signals at the BS transmitter antennas is approximately 0.216. Meanwhile, the average of the normalized squared cross correlation of the received signals at the RS antennas is approximately 0.194. This makes the adaptive PAPR reduction method utilizing the null space in the MIMO channel work better at the RS and the resultant PAPR at the RS for the same number of iterations become lower than that at the BS.

The PAPR distribution at the RS after the PAPR reduction process in Fig. 3 is better than that in Fig. 2. This is mainly due to the larger dimensions of the null space in the MIMO channel between RS and UEs as N_R is increased. To clarify this, the PAPR distribution at the RS when CF is applied at the RS is presented in Figs. 2 and 3. We see that as N_R is increased from 64 to 128, the PAPR distribution at the RS with the proposed PAPR reduction method becomes closer to that with CF. This is because the dimensions of the null space in channel $\mathbf{H}_{RU}$ are increased with a larger N_R and this makes the proposed PAPR reduction method work better at the RS. An additional reason for this is that the cross correlation of the received signals among N_R antennas at the RS becomes lower as N_R is increased, which helps the adaptive PAPR reduction utilizing the null space in the MIMO channel work better at the RS.

Figure 4 shows the average PAPR at the BS and RS as a function of N_R. Here, N_U is set to 4, T_B and T_R are set to 7 dB, and L_B and L_R are each set to 20. The average PAPR at the RS before the PAPR reduction process increases as N_R is increased. This is due to the increased variation in signal power between the antennas at the RS receiver. On the other hand, the average PAPR at the RS after the PAPR reduction process decreases as N_R is increased. This is mainly due to the larger dimensions of the null space in the MIMO channel between the RS and UEs as N_R is increased. An additional reason for this is that the cross correlation of the received signals among N_R antennas at the RS becomes lower as N_R is increased, which helps the adaptive PAPR reduction utilizing the null space in the MIMO channel work better at the RS.

Figure 5 shows the average PAPR at the BS and RS as a function of N_U. Here, N_R is set to 64, T_B and T_R are set to 7 dB, and L_B and L_R are each set to 20. The average PAPR before the PAPR reduction process decreases as N_U is increased. This is because the variation in signal power between the antennas decreases as N_U is increased. This also affects the achievable PAPR levels after the PAPR reduction process. However, since the larger N_U reduces the dimensions of the MIMO channel on the other hand, the resultant PAPR levels after the PAPR reduction process are roughly constant between the N_U values of 8 and 16.

In order to assess the computational complexity required to suppress the PAPR at the BS and RS, in Fig. 6 we show the average PAPR at the BS and RS as a function of the number of iterations, L_B and L_R. Here, N_R and N_U are set to 64 and 4, respectively. Thresholds T_B and T_R are set to 7 dB. From the figure, the PAPR decreases as L_B and L_R increase, since a more accurate PAPR reduction signal can be generated. However, the improving effect of the PAPR reduction tends to saturate as L_B or L_R increases. When comparing the PAPR levels of the BS and RS, the RS achieves the same PAPR with fewer iterations than that for the BS. This is because the cross correlation of the received signals among the RS antennas becomes lower than that for the transmission signals among the BS transmitter antennas, which helps the adaptive PAPR reduction utilizing the null space in the MIMO channel work better at the RS. This is a favorable tendency because, in general, the RS should avoid complex processing compared to that at the BS.

Figure 7 shows the average throughput as a function of the average PAPR at the RS with L_R as a parameter. Here, L_B is fixed at 20. Terms N_R and N_U are set to 64 and 4, respectively. Thresholds T_B and T_R are set to equal values, and by changing these values, the relationship between the average PAPR at the RS and the average throughput is varied. The higher the L_R is set, the higher the throughput for the same average PAPR. From this, we confirm that there is a trade-off relationship between the simplification of processing by

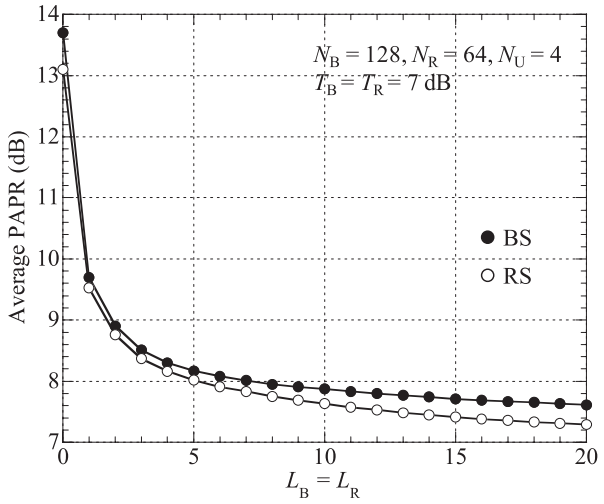

Fig. 6 Average PAPR as a function of L_B and L_R.

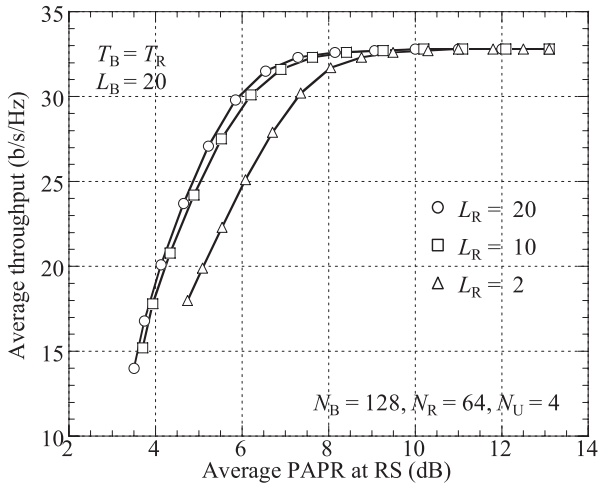

Fig. 7 Average throughput as a function of average PAPR at RS with L_R as a parameter.

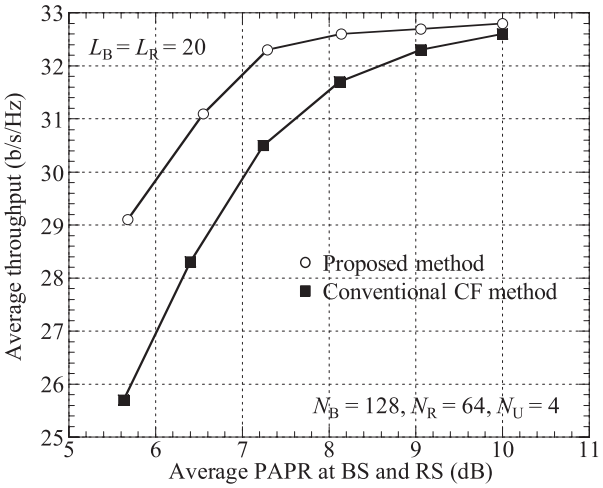

Fig. 8 Average throughput as a function of average PAPR at BS and RS.

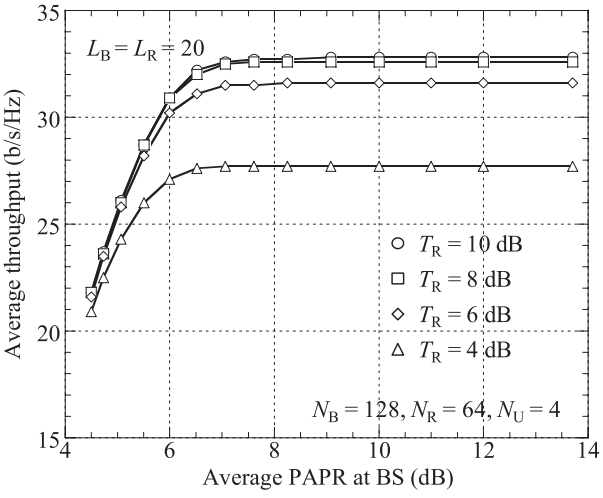

Fig. 9 Average throughput as a function of average PAPR at BS with T_R as a parameter.

reducing the number of iterations of the PAPR reduction algorithm and the PAPR vs. throughput characteristics.

Figure 8 shows the average throughput as a function of the average PAPR controlled equally at the BS and RS. Here, N_R and N_U are set to 64 and 4, respectively. The number of iterations L_B and L_R are set to 20. After adjusting power thresholds T_B and T_R so that the achievable average PAPRs at the BS and RS are the same, the relationship of the average throughput with respect to the average PAPR controlled equally at the BS and RS is traced. In addition to the proposed method that uses the adaptive PAPR reduction utilizing the null space in MIMO channels for both the BS and RS, the case where the adaptive PAPR reduction method is applied at the BS while the conventional CF is applied at the RS is tested as the conventional method. Compared to the conventional method, the proposed method significantly increases the throughput for the same PAPR value. This is because the adaptive PAPR reduction method reduces the interference from the PAPR reduction signal at the UE receiver.

Figure 9 shows the average throughput as a function of the average PAPR at the BS where power threshold T_R in the PAPR reduction at the RS is parameterized. By changing power threshold T_B in the BS, the relationship between the average PAPR at the BS and the average throughput is varied. Here, N_R and N_U are set to 64 and 4, respectively, and L_B and L_R are each set to 20. We see that as T_R is reduced to lower the PAPR at the RS, the achievable throughput for a given PAPR at the BS decreases due to the increased interference generated at the RS.

Figure 10 shows the average throughput as a function of the average PAPR at the RS when the average PAPR at the BS is parameterized. By changing power threshold T_R in the RS, the relationship between the average PAPR at the RS and average throughput is varied. Here, N_R and N_U are set to 64 and 4, respectively, and L_B and L_R are set to 20. In the region where the average PAPR required at the RS is higher than approximately 6 dB, the throughput increases as

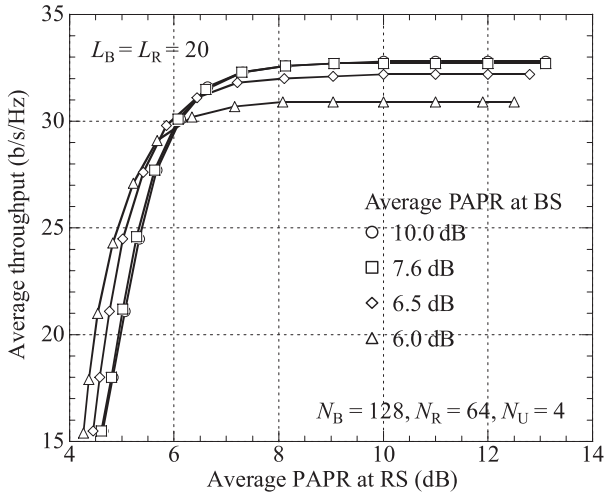

Fig. 10 Average throughput as a function of average PAPR at RS with average PAPR at BS as a parameter.

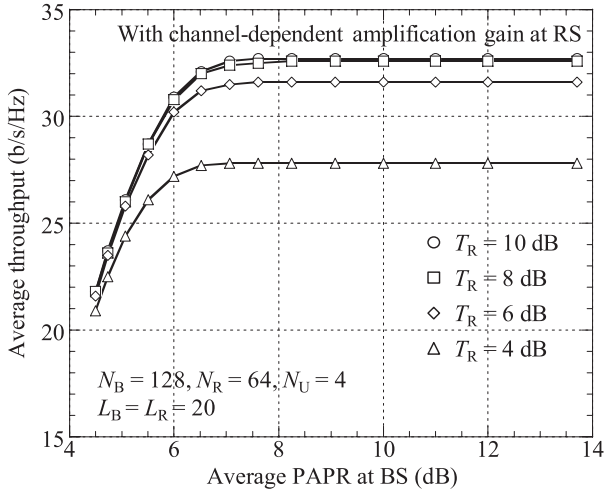

Fig. 11 Average throughput as a function of average PAPR at BS when channel-dependent amplification gain is assumed at RS.

the average PAPR at the BS increases. On the other hand, in the region where the required PAPR at the RS is less than approximately 6 dB, the lower the PAPR value at the BS is, the higher the throughput becomes. This observation suggests that when achieving a very low PAPR value in the RS, whether or not the PAPR of the transmitted signal at the BS is sufficiently suppressed in advance is important in order to reduce the interference levels generated in the PAPR reduction process of the entire system.

Figures 11 and 12 show the average throughput as a function of the average PAPR at the BS and RS, respectively, when channel-dependent amplification gain is assumed at the RS. Other settings in the evaluation in Figs. 11 and 12 are the same as those in Figs. 9 and 10, respectively. When comparing Figs. 9–12, we confirm that the proposed method works well even when we assume the channel-dependent amplification gain at the RS.

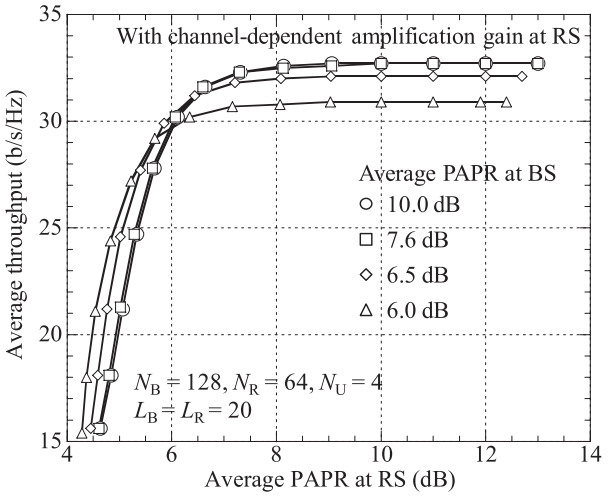

Fig. 12 Average throughput as a function of average PAPR at RS when channel-dependent amplification gain is assumed at RS.

5. Conclusion

In this paper, we proposed an adaptive PAPR reduction method utilizing the null space in MIMO channels applied to a multi-antenna AF relay transmission system. Based on computer simulation results, the proposed method suppresses the interference with the data stream due to PAPR reduction at the RS, so the average throughput for the average PAPR is significantly improved compared to the case where the conventional CF method is applied to the RS. Therefore, we expect that the proposed method can suppress the input backoff of the RS power amplifier to a low level and increase the coverage expansion effect by introducing the RS. This paper confirms the effectiveness of the application of the adaptive PAPR reduction using the null space in a MIMO channel to the multi-antenna AF-type RS. Meanwhile, the RS should avoid complex processing compared to that at the BS in general. Although the simulation results suggest that the required number of iterations in the PAPR reduction process can be reduced at the RS compared to that at the BS, further complexity reduction at the RS should be pursued as an important research subject. The implementation method of the adaptive PAPR reduction utilizing the null space in a MIMO channel in a form in which the calculation cost at the RS is smaller is left for future study.

Acknowledgments

The authors thank the reviewers for their insightful and constructive suggestions.

References

[1] T.L. Marzetta, “Noncooperative cellular wireless with unlimited numbers of base station antennas,” IEEE Trans. Wireless Commun., vol.9, no.11, pp.3590–3600, Nov. 2010.
[2] H. Papadopoulos, C. Wang, O. Bursalioglu, X. Hou, and Y.

Kishiyama, "Massive MIMO technologies and challenges towards 5G," IEICE Trans. Commun., vol.E99-B, no.3, pp.602–621, March 2016.
[3] E. Dahlman, S. Parkvall, and J. Sköld, 5G NR: The Next Generation Wireless Access Technology, Academic Press, 2018.
[4] NTT DOCOMO, White paper: 5G evolution and 6G, Jan. 2020.
[5] R.U. Nabar, H. Bolcskei, and F.W. Kneubuhler, "Fading relay channels: Performance limits and space-time signal design," IEEE J. Sel. Areas Commun., vol.22, no.6, pp.1099–1109, Aug. 2004.
[6] H. Bolcskei, R.U. Nabar, O. Oyman, and A.J. Paulraj, "Capacity scaling laws in MIMO relay networks," IEEE Trans. Wireless Commun., vol.5, no.6, pp.1433–1444, June 2006.
[7] K. Tateishi and K. Higuchi, "Adaptive amplify-and-forward relaying for cellular downlink," IEICE Trans. Commun., vol.E96-B, no.7, pp.1968–1975, July 2013.
[8] S.H. Han and J.H. Lee, "An overview of peak-to-average power ratio reduction techniques for multicarrier transmission," IEEE Wireless Commun., vol.12, no.2, pp.56–65, April 2005.
[9] X. Li and L.J. Cimini, Jr., "Effect of clipping and filtering on the performance of OFDM," IEEE Commun. Lett., vol.2, no.5, pp.131–133, May 1998.
[10] J. Armstrong, "Peak-to-average power reduction for OFDM by repeated clipping and frequency domain filtering," Electron. Lett., vol.38, no.8, pp.246–247, Feb. 2002.
[11] B.S. Krongold and D.L. Jones, "PAR reduction in OFDM via active constellation extension," IEEE Trans. Broadcast., vol.49, no.3, pp.258–268, Sept. 2003.
[12] A. Aggarwal and T.H. Meng, "Minimizing the peak-to-average power ratio of OFDM signals using convex optimization," IEEE Trans. Signal Process., vol.54, no.8, pp.3099–3110, Aug. 2006.
[13] J. Tellado and J.M. Cioffi, "Efficient algorithms for reducing PAR in multicarrier systems," Proc. IEEE Int. Symp. Inf. Theory, p.191, Cambridge, MA, Aug. 1998.
[14] H. Lee, D.N. Liu, W. Zhu, and M.P. Fitz, "Peak power reduction using a unitary rotation in multiple transmit antennas," Proc. IEEE ICC2005, pp.2407–2411, Seoul, Korea, May 2005.
[15] G.R. Woo and D.L Jones, "Peak power reduction in MIMO OFDM via active channel extension," Proc. IEEE ICC2005, pp.2636–2639, Seoul, Korea, May 2005.
[16] S. Suyama, H. Adachi, H. Suzuki, and K. Fukawa, "PAPR reduction methods for eigenmode MIMO-OFDM transmission," Proc. IEEE VTC2009-Spring, Barcelona, Spain, April 2009.
[17] H. Ando and K. Higuchi, "Comparison of PAPR reduction methods for OFDM signal with channel coding," Proc. IEEE APWCS2009, pp.139–143, Seoul, Korea, Aug. 2009.
[18] M. Eddaghel and J.A. Chambers, "PAPR reduction in distributed closed loop extended orthogonal space frequency block coding with quantized two-bit group feedback for broadband multi-node cooperative communications," Proc. IWCMC2011, pp.719–724, Istanbul, Turkey, July 2011.
[19] S. Yang, W. Yang, Y. Cai, and W. Li, "An energy efficient PTS scheme for PAPR reduction in OFDM relay systems," Proc. ChinaCom2015, pp.858–863, Shanghai, China, Aug. 2015.
[20] G. Bai, Z. Zhong, R. Xu, G. Wang, and Z. Qin, "Golay complementary sequences and Reed-Muller codes based PAPR reduction for relay networks with superimposed training," Proc. IEEE ICSP2012, pp.1558–1561, Beijing, China, Oct. 2012.
[21] Y. Sato, M. Iwasaki, S. Inoue, and K. Higuchi, "Clipping and filtering-based adaptive PAPR reduction method for precoded OFDM-MIMO signals," IEICE Trans. Commun., vol.E96-B, no.9, pp.2270–2280, Sept. 2013.
[22] S. Inoue, T. Kawamura, and K. Higuchi, "Throughput/ACLR performance of CF-based adaptive PAPR reduction method for eigenmode MIMO-OFDM signals with AMC," IEICE Trans. Commun., vol.E96-B, no.9, pp.2293–2300, Sept. 2013.
[23] T. Suzuki, M. Suzuki, Y. Kishiyama, and K. Higuchi, "Complexity-reduced adaptive PAPR reduction method using null space in MIMO channel for MIMO-OFDM signals," IEICE Trans. Commun., vol.E103-B, no.9, pp.1019–1029, Sept. 2020.
[24] T. Suzuki, M. Suzuki, and K. Higuchi, "Parallel peak cancellation signal-based PAPR reduction method using null space in MIMO channel for MIMO-OFDM transmission," IEICE Trans. Commun., vol.E104-B, no.5, pp.539–549, May 2021.
[25] H. Prabhu, O. Edfors, J. Rodrigues, L. Liu, and F. Rusek, "A low-complex peak-to-average power reduction scheme for OFDM based massive MIMO systems," Proc. ISCCSP2014, Athens, Greece, May 2014.
[26] A. Ivanov, A. Volokhatyi, D. Lakontsev, and D. Yarotsky, "Unused beam reservation for PAPR reduction in massive MIMO system," Proc. IEEE VTC2018-Spring, Porto, Portugal, June 2018.
[27] Y. Sekiguchi, N. Nonaka, and K. Higuchi, "PAPR reduction using null space in MIMO channel for MIMO-OFDM signals in multiple-antenna AF relay transmission," Proc. IEEE VTC2021-Fall, Online, Sept.-Oct. 2021.
[28] M. Sharif, M. Gharavi-Alkhansari, and B.H. Khalaj, "On the peak-to-average power of OFDM signals based on oversampling," IEEE Trans. Commun., vol.51, no.1, pp.72–78, Jan. 2003.
[29] H. Ochiai and H. Imai, "Performance analysis of deliberately clipped OFDM signals," IEEE Trans. Commun., vol.50, no.1, pp.89–101, Jan. 2002.
[30] L. Yamaguchi, N. Nonaka, and K. Higuchi, "PC-signal-based PAPR reduction using null space in MIMO channel for MIMO-OFDM signals under frequency-selective fading channel," Proc. IEEE VTC2020-Fall, Virtual conference, Nov.-Dec. 2020.

Yuki Sekiguchi received the B.E. degree from Tokyo University of Science, Noda, Japan in 2021. He is currently working towards his M.E. degree in the Department of Electrical Engineering, Tokyo University of Science, Noda, Japan. His research interests include wireless communications. He is a student member of the IEICE.

Nobuhide Nonaka received the B.E. and M.E. degrees in electronic engineering from Tokyo University of Science, Japan, in 2013 and 2015, respectively. Since April 2015, he has been with NTT DOCOMO, Inc. Since April 2018, he has been engaged in the research of next generation radio access technologies. He received the Young Researcher's Award from IEICE in 2019. He is a member of IEICE.

Kenichi Higuchi received the B.E. degree from Waseda University, Tokyo, Japan, in 1994, and received the Dr.Eng. degree from Tohoku University, Sendai, Japan in 2002. In 1994, he joined NTT Mobile Communications Network, Inc. (now, NTT DOCOMO, INC.). While with NTT DOCOMO, INC., he was engaged in the research and standardization of wireless access technologies for wideband DS-CDMA mobile radio, HSPA, LTE, and broadband wireless packet access technologies for systems beyond IMT-2000. In 2007, he joined the faculty of the Tokyo University of Science and currently holds the position of Professor. His current research interests are in the areas of wireless technologies and mobile communication systems, including advanced multiple access, radio resource allocation, inter-cell interference coordination, multiple-antenna transmission techniques, signal processing such as interference cancellation and turbo equalization, and issues related to heterogeneous networks using small cells. He was a co-recipient of the Best Paper Award of the International Symposium on Wireless Personal Multimedia Communications in 2004 and 2007, the Best Paper Award from the IEICE in 2021, a recipient of the Young Researcher's Award from the IEICE in 2003, the 5th YRP Award in 2007, the Prime Minister Invention Prize in 2010, and the Invention Prize of Commissioner of the Japan Patent Office in 2015. He is a member of the IEEE.